From free to effective diffusion coefficients in fluorescence correlation spectroscopy experiments

Emiliano Pérez Ipiña and Silvina Ponce Dawson
Departamento de Física, FCEN-UBA, and IFIBA, CONICET, Ciudad Universitaria, Pabellón I, (1428) Buenos Aires, Argentina
(Received 11 November 2012; published 13 February 2013)

Diffusion is one of the main transport processes that occur inside cells determining the spatial and time distribution of relevant action molecules. In most cases these molecules not only diffuse but also interact with others as they get transported. When these interactions occur faster than diffusion the resulting transport can be characterized by "effective diffusion coefficients" that depend on both the reaction rates and the "free" diffusion coefficients. Fluorescence correlation spectroscopy (FCS) gives information on effective rather than free diffusion coefficients under this condition. In the present paper we investigate what coefficients can be drawn from FCS experiments for a wide range of values of the ratio of reaction to diffusion time scales, using different fitting functions. We find that the effective coefficients can be inferred with relatively small errors even when the condition of fast reactions does not exactly hold. Since the diffusion time scale depends on the size of the observation volume and the reaction time scale depends on concentrations, we also discuss how by changing either one or the other property one can switch between the two limits and extract more information on the system under study.

DOI: 10.1103/PhysRevE.87.022706 PACS number(s): 87.64.−t, 87.15.R−, 87.15.Vv

I. INTRODUCTION

Diffusion plays a key role for the transport of information within and between cells. The mean square displacement of a diffusing particle is proportional to the time elapsed. This nonballistic transport is the result of the particle undergoing many (nonreacting) collisions with other (solvent) molecules (see, e.g., [1]). We identify this process as *free diffusion* and we define the *free diffusion coefficient* as the constant of proportionality that enters the ratio between the mean square displacement and time. Free diffusion coefficients can be written in terms of microscopic parameters such as the thermal velocity and the particle mean free path. Intracellular signaling agents, however, very rarely diffuse freely. Most often, they also interact with intracellular components in other ways such as binding and unbinding, i.e., they undergo *reactions*. The mean square displacement of a particle that diffuses freely and reacts is also proportional to the time elapsed if diffusion occurs on a slower time scale than reactions and the time elapsed embraces many reactive and nonreactive collisions. In this case the constant of proportionality not only depends on the parameters that characterize the microscopic movement of the particles involved but is also a function of the concentrations and reaction rates [2–4]. In this case we talk about *effective diffusion coefficients*. The effective diffusion coefficient dynamics is more complicated than that of free diffusion. On one hand, the coefficients that describe this transport depend on both parameters (free diffusion coefficients and reaction rates) and variables (concentrations) of the problem. The resulting evolution equation for the concentration of the diffusing particles is nonlinear [2,4–6] and is not exactly a diffusion equation [7]. Furthermore, it has been shown in [3] that there is not a single effective diffusion coefficient in this case. Even in the simple case with free particles P_f that diffuse with coefficient D_f and react with another species S according to the scheme

$$P_f + S \underset{k_{\text{off}}}{\overset{k_{\text{on}}}{\rightleftharpoons}} P_b, \tag{1}$$

where S is massive enough so that the S free diffusion coefficient, D_S, is the same as that of P_b and where $[S] + [P_b]$ is uniform and constant, two effective diffusion coefficients characterize the dynamics near an equilibrium situation. They are given by

$$D_t = \frac{D_f + \frac{S_{eq}}{K_D} D_S}{1 + S_{eq}/K_D} \tag{2}$$

and

$$D_u = \frac{D_f + \frac{S_{eq}^2}{K_D S_T} D_S}{1 + S_{eq}^2/(K_D S_T)}, \tag{3}$$

where $[S] = S_{eq}$, $[P_f] = P_{feq}$, and $[P_b] = P_{beq}$ are the concentrations at equilibrium, $P_T = P_{feq} + P_{beq}$ and $S_T = S_{eq} + P_{beq}$ are the total concentrations of particles and binding sites, and $K_D = k_{\text{off}}/k_{\text{on}}$ is the dissociation constant of the binding reaction (1). As mentioned before, these effective coefficients play a role when reactions occur on a faster time scale than free diffusion. In such a case, following a single particle that can be distinguished from the rest as it diffuses and reacts, one obtains the result that D_t enters the constant of proportionality between the mean square displacement and the time elapsed. D_u, on the other hand, gives the rate at which a small perturbation to the equilibrium free particle distribution diffuses out with time [3]. Thus, D_t is a *single-molecule* effective coefficient that rules the rate at which individual molecules diffuse in the medium. D_u is a *collective* effective coefficient that determines the rate at which concentration inhomogeneities spread out with time. The fact that S is significantly more massive than P_f implies that $D_S < D_f$ which, in turn, yields $D_t/D_u \leqslant 1$. Remarkably, given an equilibrium situation, this ratio can be arbitrarily small depending on the values of the equilibrium concentrations and the dissociation constant [3]. When the species P corresponds to messenger molecules, this implies that the message can travel much faster than the individual messengers [3]. For initial conditions that do not satisfy the conditions that S_T is uniform and constant, the decay back to equilibrium of the system associated with the scheme (1) is characterized by

three branches of eigenvalues (see the Appendix): two of them are purely diffusive (they correspond to D_S and D_u) and the third one can be split up into an exponential decay rate ν_{uu} and a diffusive decay rate with coefficient D_{uu}, where

$$\nu_{uu} = \left(\frac{S_{eq}}{K_D} + \frac{S_T}{S_{eq}}\right) k_{\text{off}}, \tag{4}$$

$$D_{uu} = \frac{\frac{S_{eq}^2}{K_D S_T} D_f + D_S}{1 + S_{eq}^2/(K_D S_T)}. \tag{5}$$

The fluorescent labeling of biomolecules or their expression with fluorescent tags has opened up the possibility of assessing the rate at which these molecules are transported inside cells, with minimum disruption, using optical techniques. In particular, fluorescence recovery after photobleaching (FRAP) [8–10] and fluorescence correlation spectroscopy (FCS) and its variants [11–20] are two techniques that have been widely used to determine diffusion coefficients. As shown in [3,21,22] for the model described before with the species P_f, P_b, and S that diffuse and react according to the scheme (1), FRAP yields the single-molecule effective diffusion coefficient D_t, under the assumption of fast reactions as compared to diffusion. Under the same assumption, FCS yields more than one coefficient, namely, D_S and D_u if all P_f and P_b are fluorescent and D_S, D_t, and D_u if both fluorescent and nonfluorescent particles coexist in the system [23]. In the present paper we investigate what coefficients can be drawn from FCS experiments when the condition of fast reactions does not hold. To this end we consider again the simple model with P_f, P_b, and S and, assuming that P_f and P_b are all fluorescent, we follow [23] to derive the autocorrelation function (ACF) of the fluorescence fluctuations within an observation volume. By varying the ratio of reaction to diffusion time scales we show that, as expected [15], the ACF gives the free diffusion coefficients D_f and D_S in the limit of fast diffusion and determine how the components become modified to yield D_u and D_S in the limit of fast reactions. There are various ways by which the ratio of time scales can be changed, among them, varying the observation volume or the concentrations of the species involved. We then discuss whether this variation of time scales may be achieved experimentally and, in this way, derive both free and effective diffusion coefficients in the same system. For this discussion we use parameters that give similar results to those obtained with FCS experiments performed in embryos of *Drosophila melanogaster* [24]. The aim of these experiments was to estimate the diffusion coefficient of the Bicoid protein [25], a morphogen involved in the establishment of the dorsal-ventral axis in flies [26].

II. METHODS

We consider the simple model represented by the scheme (1) where we assume that both P_f and P_b are fluorescent. The autocorrelation function of the fluorescence fluctuations in an observation volume can be expressed as the sum of three integrals. Each of these components is determined by a branch of eigenvalues of the reaction-diffusion equations that rule the dynamics of the system linearized around the equilibrium solution [13,23] (also see the Appendix). In experiments, the fluorescence is measured, and the ACF is computed and subsequently fitted to infer diffusion constants and other parameters of interest. Here we compute numerically the "full" theoretical ACF [Eqs. (A7)–(A10)] using an adaptive Lobatto quadrature algorithm (*the quadl* function of MATLAB [27]) and the parameters listed in Table I. These parameters are compatible [28,29] with the results of FCS experiments performed in embryos of *D. melanogaster* to estimate the diffusion rate of the Bicoid protein, a key morphogen for the establishment of the dorsal-ventral axis in this organism [24]. In this particular application, which should be considered merely as a platform where a generic behavior can be studied, Bicoid plays the role of the particles P_f. The values in Table I were derived from an interpretation of the fitting parameters of [24] in terms of the simple model given by Eqs. (A1). This analysis does not give an estimate of k_{off} [28,29]. Therefore, we explore a wide range of k_{off} values keeping K_D fixed. By doing this, the effective diffusion coefficients given by Eqs. (2) and (3) remain fixed at $D_t = 7.3\ \mu\text{m}^2\,\text{s}^{-1}$ and $D_u = 8.8\ \mu\text{m}^2\,\text{s}^{-1}$. With this exploration, on the other hand, we can analyze the behavior of the ACF outside the fast reaction limit. Although the simple model considered here with the parameters of the table reproduces the ACF obtained from FCS experiments in [24], assuming that all Bicoid (Bcd) molecules are fluorescent is not realistic [28,29]. A better interpretation of the experimental results of [24] is obtained when the simple model is extended to assume that both fluorescent and nonfluorescent Bcd molecules coexist in the system [29]. Thus, the simple model analyzed here with the parameters of Table I should be mainly considered as an illustrative example in which the behavior of the ACF in different limits can be explored.

TABLE I. Biophysical and photophysical parameters used to generate the full ACF given by Eqs. (A7)–(A10). The dissociation constant k_{off} is varied within the range displayed in the table. The values of k_{on} are varied accordingly to keep K_D fixed. This guarantees that the effective diffusion coefficients of Eqs. (2), (3), and (5) also remain fixed at $D_t = 7.3\ \mu\text{m}^2\,\text{s}^{-1}$, $D_u = 8.8\ \mu\text{m}^2\,\text{s}^{-1}$, and $D_{uu} = 10.6\ \mu\text{m}^2\,\text{s}^{-1}$.

Biophysical parameters	
D_f	$19\ \mu\text{m}^2\,\text{s}^{-1}$
D_S	$0.38\ \mu\text{m}^2\,\text{s}^{-1}$
P_T	35 nM
S_T	77 nM
K_D	32 nM
k_{off}	$\in [10^{-4}\ \text{s}^{-1}, 10^5\ \text{s}^{-1}]$
Photophysical parameters	
w_r	$0.4\ \mu\text{m}$
w	5
V_{eff}	$1.78\ \mu\text{m}^3$

Once the full ACF G is computed we try to fit it using different approximate expressions $\tilde{G}$, from which we determine weights $\tilde{G}_{o_i}$, diffusive times $\tilde{\tau}_i$, and, depending on the expression, other fitting parameters. From the times, we derive diffusion coefficients $\tilde{D}_i = w_r^2/(4\tilde{\tau}_i)$, assuming known values of w_r, w, and V_{eff} as listed in Table I.

For the fitting we try forms that are often used to analyze FCS data sets obtained from experiments. We first try a superposition of two terms with the same τ dependence as the one encountered in the case of free diffusion,

$$G(\tau) \approx \tilde{G}(\tau) = \sum_{i=1}^{2} \frac{\tilde{G}_{o_i}}{\left(1+\frac{\tau}{\tilde{\tau}_i}\right)\sqrt{1+\frac{\tau}{w^2\tilde{\tau}_i}}} \tag{6}$$

because it embraces both the fast diffusion Eq. (A6) and the fast reaction Eq. (A15) approximations. Being able to fit the ACF with such an expression does not mean that free diffusion is the only process that is taking place in the system. In fact, in the fast reaction limit the ACF is of this form but with one of the characteristic time scales corresponding to an effective, not a free, diffusion coefficient.

We then try an expression of the form

$$G(\tau) \approx \tilde{G}(\tau) = \frac{\tilde{G}_{o_1}}{\left(1+\frac{\tau}{\tilde{\tau}_1}\right)\sqrt{1+\frac{\tau}{w^2\tilde{\tau}_i}}} + \frac{\tilde{G}_{o_2}}{\left(1+\frac{\tau}{\tilde{\tau}_2}\right)\sqrt{1+w^2\frac{\tau}{w^2\tilde{\tau}_2}}} + \frac{\tilde{G}_{o_3}}{\left(1+\frac{\tau}{\tilde{\tau}_3}\right)\sqrt{1+\frac{\tau}{w^2\tilde{\tau}_3}}} e^{-\tilde{\nu}\tau}, \tag{7}$$

where $\tilde{\nu}$ is an additional fitting parameter. In this case, the ACF has three components, two of which have a diffusive τ dependence while the third one has in addition an exponentially decaying factor. We have tried this combination because it corresponds to the behavior encountered for the eigenvalues of the linearized problem in the limit of small wave number [see Eqs. (A13) and (A14)]. An ACF with the τ dependence of Eq. (7), on the other hand, is the one used in [18] to analyze a system in which the species undergo free diffusion and reactions.

We have also probed a superposition of two components such as the ones that are used for experiments in which the fluorescent molecules undergo anomalous diffusion [30],

$$G(\tau) \approx \tilde{G}(\tau) = \sum_{i=1}^{2} \frac{\tilde{G}_{o_i}}{\left[1+\left(\frac{\tau}{\tilde{\tau}_i}\right)^{\tilde{\alpha}_i}\right]\sqrt{1+w^{-2}\left(\frac{\tau}{\tilde{\tau}_i}\right)^{\tilde{\alpha}_i}}}. \tag{8}$$

with the $\tilde{\alpha}_i$'s free fitting parameters. We do not show the details of the results obtained in this case.

Finally, we also seek to fit each of the three components of the full ACF separately by an expression of the form

$$\tilde{G}_i(\tau) = \frac{\tilde{G}_{o_i}}{\left(1+\frac{\tau}{\tilde{\tau}_i}\right)\sqrt{1+\frac{\tau}{w^2\tilde{\tau}_i}}} e^{-\tilde{\nu}_i\tau}. \tag{9}$$

Since we have an analytic expression for the first component G_1 [Eq. (A8)], we do not perform the fitting but directly set $\tilde{G}_{o_1} = G_{os}$, $\tilde{\tau}_1 = \tau_s = w_r^2/(4D_S)$, and $\tilde{\nu}_1 = 0$.

In order to obtain the fitting parameters we minimize the difference $|G - \tilde{G}|$ using a nonlinear least squares method for the minimization (a trust region reflective algorithm, the *lsqcurvefit* function of MATLAB [27]). The goodness of the fitting is evaluated by computing the χ^2:

$$\chi^2 = \sum_j [G(t_j) - \tilde{G}(t_j)]^2, \tag{10}$$

with $\{t_j\}$ the times for which both G and $\tilde{G}$ are computed. The total numbers of degrees of freedom in the three cases probed are very similar (they are mainly determined by the number of data points that we use for the fitting). Penalizing the χ^2 in view of the different numbers of fitting parameters does not introduce noticeable changes and we do not take them into account when comparing the goodness of the fit.

We also perform some stochastic simulations to mimic the situation encountered in FCS experiments. More specifically, we consider a rectangular volume of sides L_x, L_y, and L_z with $L_y = L_x = L$ and $L_z = 5L$, which we divide using the same grid spacing Δr in all directions. Δr and the time step Δt are chosen as $\Delta t \leqslant \tau_r \equiv 1/[k_{\text{off}}(1 + P_{feq}/K_D + S_{eq}/K_D)]$ and $\Delta t \leqslant \Delta r^2/(6D_f)$. The figures shown in this paper were drawn using $L = 10\ \mu$m, $\Delta t = 22\ \mu$s, and $\Delta r = 0.05$–$0.16\ \mu$m. Given the volume of the simulation, we choose the total number of particles of each species so that their concentrations correspond to the values of Table I. The fraction of bound particles and of bound traps is chosen so as to satisfy the equilibrium conditions [Eq. (A2)]. All molecules are initially distributed with uniform probability over the grid points. Each molecule is moved to one of its six neighboring points with equal probability every $n_D = \Delta r^2/(6D\Delta t)$ time steps, where D is the free diffusion coefficient of the molecule. We use reflecting boundary conditions at the border. At every time step, after all the corresponding random walks are performed, the occurrence of the binding reactions is decided for each pair of free particles and free traps that are at the same grid point with probability $p_{\text{on}} = (k_{\text{on}}\Delta t \times 10^{21}\ \mu\text{M}\,\mu\text{m}^3)/(\Delta r^3 N_A)$ where N_A is Avogadro's number. Once a new bound particle P_b is formed, the time it will remain bound (i.e., as P_b) is randomly chosen from an exponential distribution of mean $1/k_{\text{off}}$. The same procedure is applied at $t = 0$ with all bound particles. This means that the simulation assigns a lifetime to every bound particle. Thus, at each time step, after the decision on the binding reactions is made, it is checked whether there are any molecules P_b that are supposed to unbind at that particular time and the unbinding is performed. All the simulations for which results are shown in this paper were run for a total time $t = 200$ s. Finally, the total fluorescence as a function of time is computed according to

$$F(t) = \int QI(\mathbf{r})\{[P_f](\mathbf{r},t) + [P_b](\mathbf{r},t)\}d^3r, \tag{11}$$

with $Q = 1$, $[P_f](\mathbf{r},t) = \sum_{if} \delta(\mathbf{r} - \mathbf{r}_{if}(t))$, and $[P_b](\mathbf{r},t) = \sum_{ib} \delta(\mathbf{r} - \mathbf{r}_{ib}(t))$, where $\mathbf{r}_{if}(t)$ and $\mathbf{r}_{ib}(t)$ are the locations of the free and bound particles at time t, respectively, and $I(\mathbf{r})$ the intensity distribution of the illumination spot which is approximated as a three-dimensional Gaussian distribution. Using the total fluorescence the ACF is computed as is done with an experimental record. Notice that Q scales out from the ACF so that its actual value is irrelevant for our purposes.

III. RESULTS

A. The full ACF in different limits

In order to study how the full ACF behaves outside the fast reaction limit we computed it for the wide range of k_{off} values described in Table I. For the parameters used, the particle free

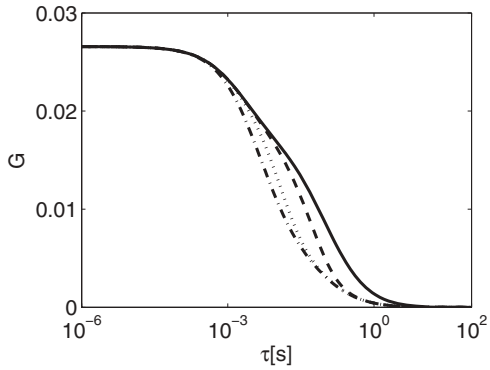

FIG. 1. Full ACF computed numerically using the parameter values of Table I and $k_{\rm off} = 10^{-3}$ s^{-1} (solid line), $k_{\rm off} = 10$ s^{-1} (dashed line), $k_{\rm off} = 100$ s^{-1} (dotted line), and $k_{\rm off} = 10^{-5}$ s^{-1} (dash-dotted line). The ACFs for $k_{\rm off} \leqslant 1/$s are almost indistinguishable from the one with $k_{\rm off} = 10^{-3}$ s^{-1}. Something similar happens for those with $k_{\rm off} \geqslant 1000/$s and the one for $k_{\rm off} = 10^5$ s^{-1}. These extreme behaviors are associated with two different limits: the fast diffusion limit (small $k_{\rm off}$) and the fast reaction limit (large $k_{\rm off}$).

diffusion time scale is $\tau_f = w_r^2/(4D_f) = 2 \times 10^{-3}$ s [or $\tau_f = (ww_r)^2/(4D_f) = 5 \times 10^{-2}$ s if we consider the characteristic length scale $w_z = ww_r$ along the axis of observation] while the reaction time scale $\tau_r = 1/[k_{\rm off}(1 + P_{feq}/K_D + S_{eq}/K_D)]$ varies between 3.23×10^{-6} and 3.23×10^3 s ($\tau_r = 0.32\, k_{\rm off}^{-1}$). In this way we go from the fast reaction to the fast diffusion limit ($\tau_f \ll \tau_r$). These two limits become clear in Fig. 1 where we have plotted four of the various curves obtained. The existence of two time scales, one of which is of the order of 10^{-1} s, seems apparent in the two limits. For the scale of the figure, both limiting curves ($k_{\rm off} = 10^5$ s^{-1} plotted with the dash-dotted line and $k_{\rm off} = 10^{-3}$ s^{-1} plotted with the solid line) are indistinguishable for $\tau > 10$ s and $\tau < 10^{-4}$ s. Furthermore, most of the curves obtained are well described by either limit in the middle region $10^{-4} < \tau < 10$ s with a slight discrepancy for $\tau \sim 1$ s (data not shown). The two curves that do not seem to approach either of the two limits in the middle region are the other two that we have plotted in Fig. 1, which correspond to $k_{\rm off} = 10$ s^{-1} (dashed line) and $k_{\rm off} = 100$ s^{-1} (dotted line).

We then tried to fit the various curves using the models described in Sec. II. We show the fitting parameters and the corresponding χ^2 values obtained in Tables II and III. The weights are listed in terms of their fraction with respect to their sum, $\tilde{G}_o$, which satisfies $\tilde{G}_o = \tilde{G}(\tau = 0)$. We show the differences between the full and the fitted ACFs for some values of $k_{\rm off}$ in Fig. 2. As shown in Fig. 2(a), the difference between the full ACF and the fitting function given by Eq. (6) is negligible for large and small values of $k_{\rm off}$ ($k_{\rm off} \gg 100/$s and $k_{\rm off} \ll 10/$s, respectively). For intermediate values, $10/\text{s} \leqslant k_{\rm off} \leqslant 100/$s, the fitting is not as good but the difference never exceeds 10% of the full ACF in the relevant region of τ ($\tau \leqslant 0.1$ s). When looking at the values of the fitting parameters (see Table II), we observe a transition from a situation in which one of the estimated diffusion coefficients is $\tilde{D}_2 \sim 19\ \mu$m^2/s to a situation in which it is $\tilde{D}_2 \sim 8.5\ \mu$m^2/s as $k_{\rm off}$ is increased. $\tilde{D}_1$ does not vary significantly, $\tilde{D}_1 \sim 0.4\ \mu$m^2/s, for most values of $k_{\rm off}$. $\tilde{D}_1$ corresponds to the free diffusion coefficient of the binding sites, $D_S = 0.38\ \mu$m^2/s. For large $k_{\rm off}$ (i.e., for fast reactions), $\tilde{D}_2 \approx D_u = 8.8\ \mu$m^2. Both the times and the weights agree with those of the analytic approximation in the fast reaction limit [23] (also see the Appendix). For small $k_{\rm off}$, $\tilde{D}_2 \approx D_f = 19\ \mu$m^2/s, the free diffusion coefficient of the particles. In this case we recover the results of the analytic approximation to the ACF in the fast diffusion limit [15] (also see the Appendix). In between these two limits the solution to the minimization problem gives a value $\tilde{D}_1$ that differs by up to a factor of 3 with respect to the free coefficient of the binding sites. $\tilde{D}_2$ stays close to either one of the values D_f and D_u obtained in each limit for almost all values of $k_{\rm off}$. The exception is $k_{\rm off} = 10/$s for which $\tilde{D}_2$

TABLE II. Parameters obtained using expression (6) to fit the full ACF for various values of $k_{\rm off}$ and corresponding χ^2 values. The smaller the χ^2 the better the fitting is. In the limit of fast reactions, $k_{\rm off} > 100$ s^{-1}, the parameters agree with those of [23]. In the limit of fast diffusion, $k_{\rm off} \leqslant 10^{-1}$ s^{-1}, the estimated diffusion rates are similar to the free diffusion coefficients, $D_f = 19\ \mu$m^2/s and $D_S = 0.38\ \mu$m^2/s.

$k_{\rm off}$ ($\frac{1}{\rm s}$)	$\frac{\chi^2}{10^{-8}}$	$\tilde{D}_1$ ($\frac{\mu\rm m^2}{\rm s}$)	$\tilde{D}_2$ ($\frac{\mu\rm m^2}{\rm s}$)	$\frac{\tilde{G}_{o1}}{\tilde{G}_o}$	$\frac{\tilde{G}_{o2}}{\tilde{G}_o}$
0.0001	1.26	0.38	18.95	0.63	0.37
0.001	1.28	0.38	18.96	0.63	0.37
0.01	1.70	0.38	19.00	0.63	0.37
0.1	18.0	0.40	19.43	0.64	0.36
1	320	0.50	22.31	0.67	0.33
5	645	0.82	27.92	0.72	0.28
10	495	1.08	30.96	0.75	0.25
25	177	1.59	33.10	0.79	0.21
50	249	2.00	28.20	0.79	0.21
100	587	1.16	7.82	0.39	0.61
250	126	0.31	6.36	0.14	0.86
500	320	0.31	7.10	0.15	0.85
1000	7.37	0.33	7.71	0.16	0.84
10000	0.73	0.37	8.57	0.18	0.82
100000	0.41	0.38	8.68	0.18	0.82

TABLE III. Similar to Table II but using expression (7) to fit the full ACF. All quantities measured with the same units as in Table II.

$k_{\rm off}$	$\frac{\chi^2}{10^{-9}}$	$\tilde{D}_1$	$\tilde{D}_2$	$\tilde{D}_3$	$\tilde{\nu}^{-1}$	$\frac{\tilde{G}_{o1}}{\tilde{G}_o}$	$\frac{\tilde{G}_{o2}}{\tilde{G}_o}$	$\frac{\tilde{G}_{o3}}{\tilde{G}_o}$
0.0001	8.12		18.95	0.38	28.54	0.00	0.37	0.63
0.001	8.02		18.95	0.38	28.51	0.00	0.37	0.63
0.01	6.98		18.94	0.38	25.93	0.00	0.37	0.63
0.1	2.32		18.96	0.38	11.00	0.00	0.36	0.64
1	4.70	0.39	19.10	0.37	0.76	0.21	0.36	0.43
5	11.5	0.48	19.72	0.31	0.15	0.26	0.35	0.39
10	14.5	0.56	20.33	0.25	0.08	0.31	0.34	0.36
25	18.1	0.60	21.66	0.21	0.03	0.31	0.31	0.38
50	23.5	0.60	23.73	0.51	0.02	0.31	0.26	0.43
100	35.0	0.61	28.55	1.54	0.02	0.31	0.19	0.50
250	51.2	0.62	54.14	4.30	0.02	0.32	0.06	0.62
500	49.1	0.61	140.8	6.28	0.02	0.31	0.01	0.68
1000	33.3	0.34	4.42	9.30	0.01	0.15	0.53	0.31
10000	2.65	0.38	8.34			0.18	0.80	0.02
100000	2.60	0.38	8.53			0.18	0.81	0.01

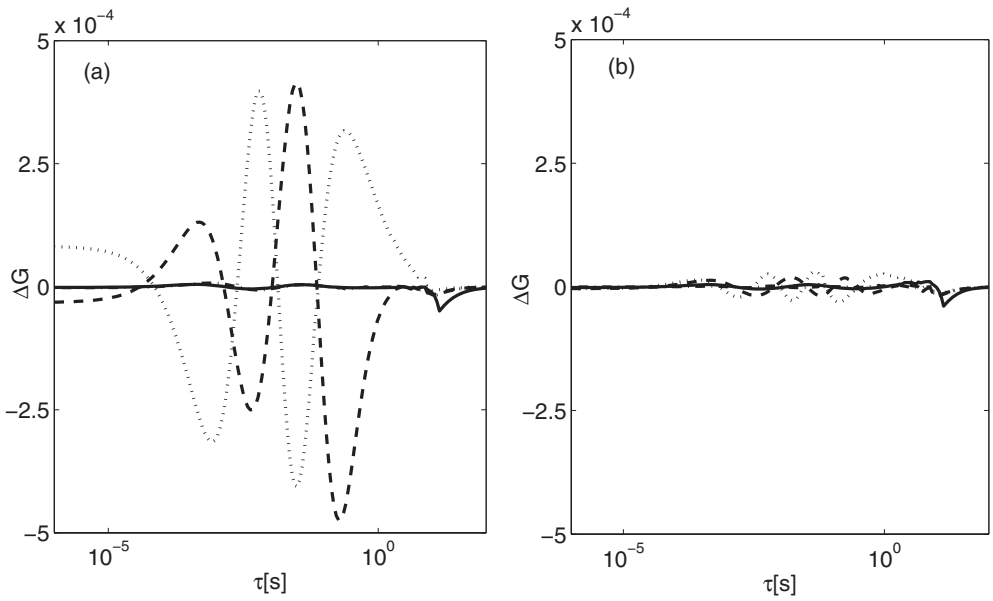

FIG. 2. Difference ΔG between the full ACF and the approximated models with which we tried to fit it for $k_{\rm off} = 0.001/\rm s$ (solid line), $k_{\rm off} = 10/\rm s$ (dashed line), $k_{\rm off} = 100/\rm s$ (dotted line), and $k_{\rm off} = 10^5/\rm s$ (dash-dotted line). (a) The model given by Eq. (6). (b) The model given by Eq. (7). In all cases ΔG is negligible for small and large values of $k_{\rm off}$ while for intermediate values the differences get larger although they never exceed 10% of the full ACF for $\tau \leqslant 0.1$ s.

is 1.5 times larger than D_f. This value of $k_{\rm off}$ corresponds to $\tau_r \approx 0.03$ s which is of the order of the value of τ_f that is obtained using the longest length scale of the observation volume [$\tau_f = (ww_r)^2/(4D_f) = 0.05$ s].

Fitting the full ACF with the model given by Eq. (7) gives very small differences all across the range of $k_{\rm off}$ values that we tested [see Fig. 2(c)]. For $k_{\rm off} \geqslant 10^4/\rm s$ the weight of the component with the exponential decay, G_{o_3}, is zero and the model coincides with the one given by Eq. (6). The diffusion coefficients obtained in this case are the free diffusion coefficient of the binding sites, D_S, and the effective diffusion coefficient, D_u, as predicted by the fast reaction approximation [23] (also see the Appendix). For $k_{\rm off} \leqslant 0.1/\rm s$, the weight G_{o_1} becomes zero. As may be observed in Table III, for $k_{\rm off} \leqslant 0.1/\rm s$ the characteristic decay time $\tilde{\nu}^{-1}$ associated with the third component of (7) is much larger than all the other characteristic times [$\tilde{\nu}^{-1} \gg \tau_{\rm max} = w_r^2/(4D_{\rm min}) \sim 0.1$ s]. Furthermore, it corresponds to a time at which the ACF is about 10% of its maximum value. Therefore, $\exp(-\tilde{\nu}\tau) \approx 1$ for $\tau \leqslant 0.1$ s and the fitting function Eq. (7) is approximately of the same form as Eq. (6) in the relevant region of τ. The diffusion coefficients obtained for $k_{\rm off} \leqslant 0.1/\rm s$ are approximately equal to the free coefficients D_f and D_S. For $0.1/\rm s < k_{\rm off} \leqslant 1000/\rm s$ fitting the ACF with this model gives smaller errors than with the other two models. However, the fitted diffusion coefficients cannot always be related to an actual coefficient of the problem (e.g., compare the values obtained for $k_{\rm off} = 1000/\rm s$ with those described in the caption to Table I). Furthermore, although for $k_{\rm off} \leqslant 1/\rm s$ or $k_{\rm off} \geqslant 10^4/\rm s$ a purely diffusive term with the free coefficient of the trap is found with this fitting (it is embraced by $\tilde{G}_3$ for $k_{\rm off} \leqslant 0.1/\rm s$, and it corresponds to $\tilde{G}_1$ for $k_{\rm off} = 1/\rm s$ and $k_{\rm off} \geqslant 10^4/\rm s$), no such term is found for $10/\rm s \leqslant k_{\rm off} \leqslant 100/\rm s$. Such a term should always be present as explained in the Appendix. It is found with a ~10% error at $k_{\rm off} = 10^3/\rm s$, but the other coefficients are not meaningful. For $k_{\rm off} \geqslant 10^4/\rm s$ this fitting gives the same results as those of Eqs. (6) in the fast reaction limit with $\tilde{D}_1 \approx D_S$ and $\tilde{D}_2 \approx D_u$.

B. Components of the ACF

In order to understand the transition from the fast diffusion to the fast reaction limit, we analyzed the behavior of the three components of the full ACF [see Eqs. (A8)–(A10)], for different values of $k_{\rm off}$. As explained in more detail in the Appendix, each component corresponds to the eigenvalue of a linear problem and is characterized by a time scale. The first of these eigenvalues does not depend on $k_{\rm off}$ and its associated component, for which we have an analytic expression, remains unchanged for all values of $k_{\rm off}$. This does not hold for the other two components for which we do not have an analytic expression and which depend strongly on $k_{\rm off}$. To study their behavior we determined them by numerical integration. We show the results in Fig. 3 where we have plotted the three components for increasing values of $k_{\rm off}$ from Fig. 3(a) to Fig. 3(d). We show in Fig. 4 the characteristic times and weights obtained by fitting each component G_i separately for each value of $k_{\rm off}$ probed using the expression given by Eq. (9). We observe that, in the fast diffusion limit [Fig. 3(a)], both G_1 and G_2 have approximately the same correlation time. This can be verified in Fig. 4(a) where we observe that they are both characterized by the same diffusion coefficient, which corresponds to the free coefficient of the binding sites ($\tilde{D}_1 \approx \tilde{D}_2 \approx D_S$) for $k_{\rm off} \leqslant 1\ \rm s^{-1}$. The fit of the second component G_2 not only gives a diffusive time scale [shown in Fig. 4(a)] but also a time scale associated with an exponential decay [$\tilde{\nu}_2^{-1}$ displayed in Fig. 4(b)]. This characteristic time scale is at least an order of magnitude larger than that of diffusion ($\tilde{\nu}_2^{-1} \geqslant 0.78$ s and $\tilde{\tau}_2 \sim 0.1$ s for $k_{\rm off} \leqslant 1\ \rm s^{-1}$). Thus,

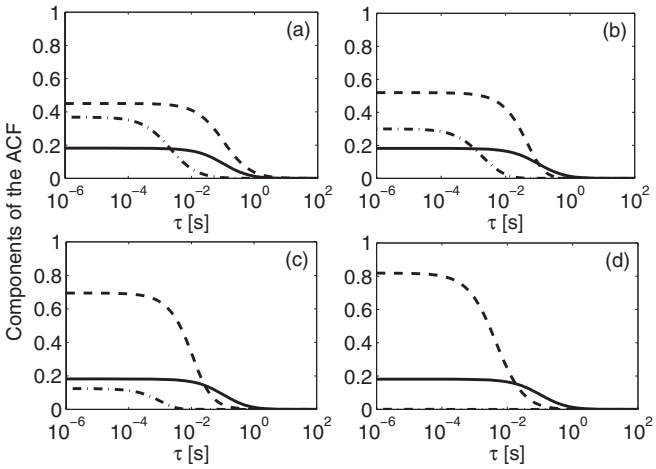

FIG. 3. Components of the full ACF for different values of $k_{\rm off}$ normalized to the sum of all the weights, $G_o \equiv \sum_{i=1}^{3} G_i(\tau = 0)$: G_1/G_o (solid line), G_2/G_o (dashed line), and G_3/G_o (dash-dotted line). (a) $k_{\rm off} = 10^{-3}$ s^{-1}, which corresponds to the limit of fast diffusion. G_1 and G_2 decay at approximately the same time so they prescribe the same diffusion coefficient, which is the free coefficient of the binding sites, $D_1 = D_2 = D_S$. (b) $k_{\rm off} = 10$ s^{-1}. In this case the characteristic time of the component G_2 is smaller than in (a). (c) $k_{\rm off} = 10^2$ s^{-1}. In this case, the relative weight of G_2 is larger than in (b) while that of G_3 decreases. The characteristic time of G_2 is smaller than in (b). (d) $k_{\rm off} = 10^5$ s^{-1}, which corresponds to the limit of fast reactions. In this case the relative weight of the component G_3 becomes negligible.

the decay of G_2 is dominated by diffusion and it is the free diffusion coefficient of the binding sites that determines the characteristic time of this decay. This becomes clear in Fig. 3(a) where we can observe that G_2 is negligible for $\tau \sim \tilde{\nu}_2^{-1}(k_{\rm off} = 10^{-3}\ {\rm s}^{-1}) = 250$ s. In this regard, something similar happens to G_3, for which $\tilde{\nu}_3^{-1} \geqslant 0.13$ s while $\tilde{\tau}_3 \sim 2.1 \times 10^{-3}$ s

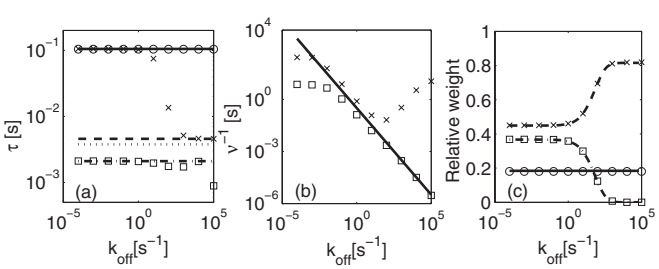

FIG. 4. Characteristic times and weights obtained by fitting each component G_i of the full ACF separately using an expression of the form (9). Since we have an analytic expression for the first component (see the Appendix) we do not perform the fitting but plot the corresponding parameter values directly. (a) Fitted diffusion times $\tilde{\tau}_1$ (open circles), $\tilde{\tau}_2$ (crosses), $\tilde{\tau}_3$ (open squares), and analytic diffusion times $\tau_S = w_r^2/(4D_S)$ (solid line), $\tau_u = w_r^2/(4D_u)$ (dashed line), $\tau_{uu} = w_r^2/(4D_{uu})$ (dotted line), and $\tau_f = w_r^2/(4D_f)$ (dash-dotted line). (b) Times that characterize the exponential decay, those obtained from the fitted $\tilde{\nu}_2^{-1}$ (crosses) and $\tilde{\nu}_3^{-1}$ (open squares) and the analytic one ν_{uu}^{-1} given by Eq. (4) (solid line). (c) Relative weights G_{o_1}/G_o (solid line), G_{o_2}/G_o (dashed line), and G_{o_3}/G_o (dash-dotted line) with their fitted values in marks.

for $k_{\rm off} \leqslant 1$ s^{-1}. Thus, for $k_{\rm off} \leqslant 1$ s^{-1} the decay of G_3 is dominated by diffusion and the corresponding characteristic time is that of the free particle diffusion coefficient D_f, as may be observed in Fig. 4(a). Therefore, for $k_{\rm off} \leqslant 1/$s, by fitting each component separately we obtain that the ACF is basically the sum of two purely diffusive components with the free diffusion coefficients of the binding sites and of the particles. This indicates that the fast diffusion limit holds up to $k_{\rm off} = 1/$s for which $\tau_r = 0.32$ s while $\tau_f = w_r^2/(4D_f) = 2 \times 10^{-3}$ s [or $\tau_f = (ww_r)^2/(4D_f) = 5 \times 10^{-2}$ s if we consider the characteristic length scale $w_z = ww_r$]. The situation described so far apparently is not very different from the one encountered for $k_{\rm off} = 10/$s, for which $\tilde{\nu}_2^{-1} = 0.12$ s, $\tau_2 = 0.075$ s, $\tilde{\nu}_3^{-1} = 0.016$ s, and $\tau_3 = 0.002$ s. This could be an indication that the ACF could be fitted by the sum of two purely diffusive terms characterized by the free diffusion coefficients D_S and D_f. However, the χ^2 obtained for the fit to G_2 at $k_{\rm off} = 10/$s is much larger than the ones obtained for $k_{\rm off} \leqslant 1/$s. In fact, when we try to fit with two diffusive components the ACF obtained for $k_{\rm off} = 10/$s we do not converge to the free diffusion coefficients (see Table II). As $k_{\rm off}$ is increased (i.e., as the reactions become faster), the characteristic decay time of G_2 decreases (the diffusion coefficient increases) while the relative weight of this component increases (see Figs. 3(b), 3(c), and 4). For $k_{\rm off} = 100/$s, fitting each component separately gives results that are not purely diffusive. Namely, for both G_2 and G_3 the exponentially decaying term becomes relevant since the corresponding characteristic times are not much larger than those of diffusion ($\tilde{\nu}_2^{-1} = 6.7 \times 10^{-2}$ s, $\tilde{\tau}_2 = 1.4 \times 10^{-2}$ s, $\tilde{\nu}_3^{-1} = 2.95 \times 10^{-3}$ s, $\tilde{\tau}_3 = 1.74 \times 10^{-3}$ s). On the other hand, although $\tilde{D}_3 \approx D_f$, $\tilde{D}_2$ is different from all the coefficients with which we can associate a biophysical meaning within the model used. The χ^2, however, is larger than for $k_{\rm off} \leqslant 1/$s. Thus, the fitting is not as good. For $k_{\rm off} \geqslant 10^3$ s^{-1} the relative weight G_{o_3}/G_o is negligible [Figs. 3(d) and 4(c)] and G_2 is described by a purely diffusive term ($\tilde{\tau}_2 \sim 5 \times 10^{-3}$ while $\tilde{\nu}_2 \geqslant 0.33$ s) that is characterized by the effective diffusion coefficient D_u of Eq. (3), which satisfies $D_S \leqslant D_u \leqslant D_f$ as shown in Fig. 4(a).

C. Dependence of the fitted diffusion coefficients on concentrations

The ACF of the example considered here gives two diffusion coefficients in the limits of fast diffusion and of fast reactions. An important difference between the two limiting cases is the type of coefficients that are obtained: they are both free in the former and one of them is effective in the latter. Effective diffusion coefficients depend on concentrations and reaction rates. In order to check that this is the case for the coefficients that we derive from the fitting, we computed the ACF for the parameters of Table I using different values of P_T and $k_{\rm off}$. Given that the reaction characteristic time is given by $\tau_r = (k_{\rm off} + k_{\rm on}P_{feq} + k_{\rm on}S_{eq})^{-1}$, varying the concentrations can change the relationship between τ_r and the free diffusion time $\tau_f = w_r^2/(4D_f)$. The curves in Fig. 5 were obtained choosing values of $k_{\rm off}$ that allow the concentration of P_T to be changed, keeping the same type of relation between τ_f and τ_r all across each subfigure. Namely, $\tau_f = 2 \times 10^{-3}$ s for all

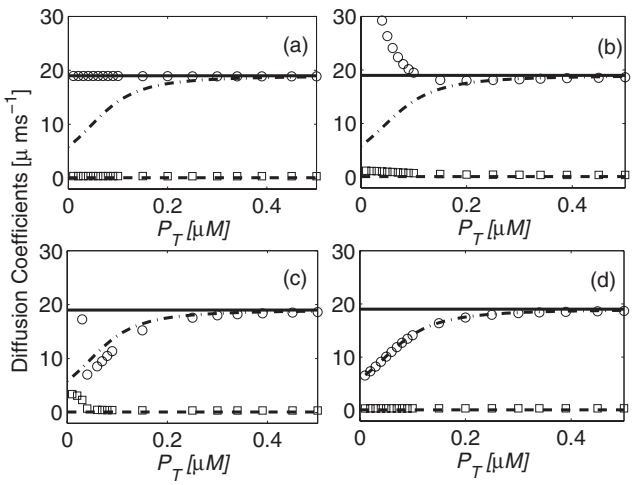

FIG. 5. Diffusion coefficients derived by fitting ACFs obtained for different values of P_T and $k_{\rm off}$ with an expression of the form (6) ($\tilde{D}_1$, open squares; $\tilde{D}_2$, open circles) and characteristic diffusion coefficients of the problem (D_S, dashed line; D_u, dash-dotted line; D_f, solid line). (a) $k_{\rm off} = 10^{-5}$ s^{-1}, which corresponds to the fast diffusion limit. Neither $\tilde{D}_1$ nor $\tilde{D}_2$ varies with P_T and they coincide with the free coefficients of the problem. (b) $k_{\rm off} = 10$ s^{-1} and $3.1 \leqslant \tau_r/\tau_f \leqslant 38$. (c) $k_{\rm off} = 100$ s^{-1} and $0.31 \leqslant \tau_r/\tau_f \leqslant 3.8$. (d) $k_{\rm off} = 10^6$ s^{-1}, which corresponds to the fast reaction limit. $\tilde{D}_1$ does not change with P_T and satisfies $\tilde{D}_1 \approx D_S$. $\tilde{D}_2$ does change with P_T and satisfies $\tilde{D}_2 \approx D_u$.

subfigures while $6.2 \times 10^2 \leqslant \tau_r \leqslant 7.6 \times 10^3$ s in Fig. 5(a), $6.2 \times 10^{-3} \leqslant \tau_r \leqslant 7.6 \times 10^{-2}$ s in Fig. 5(b), $6.2 \times 10^{-4} \leqslant \tau_r \leqslant 7.6 \times 10^{-3}$ s in Fig. 5(c), and $6.2 \times 10^{-7} \leqslant \tau_r \leqslant 7.6 \times 10^{-6}$ s in Fig. 5(d), with τ_r decreasing with increasing P_T. We show in Fig. 5 (with symbols) the diffusion coefficients derived by fitting the ACFs obtained for different values of P_T and $k_{\rm off}$ with an expression of the form (6). The plots of Figs. 5(a) and 5(d) illustrate the fast diffusion and the fast reaction limits. Figures 5(b) and 5(c) correspond to intermediate cases. We observe in Fig. 5(a) that neither of the coefficients derived from the ACF changes with P_T, i.e., they are both free coefficients. Furthermore, they agree with the expected values D_S and D_f (shown with curves). We observe in Fig. 5(d) that $\tilde{D}_1$ remains constant (and approximately equal to D_S) while $\tilde{D}_2$ increases with P_T. We also observe that $\tilde{D}_2 \approx D_u$ for the whole range of P_T values explored. Both $\tilde{D}_2$ and D_u approach D_f as P_T increases. This is so because, as P_T increases, the binding sites eventually become saturated and most of the particles diffuse freely. This shows that, even in the fast reaction limit, the free diffusion coefficient D_f can be recovered, depending on the relative concentrations of the reactants at work. We observe in Figs. 5(b) and 5(c) that even outside the fast reaction limit (when τ_f is slightly smaller than or of the order of τ_r) fitting the ACF with two diffusive components gives relatively good estimates of D_S and D_u. This is so for $P_T \geqslant 0.15$ μM in Fig. 5(b), which corresponds to $\tau_r/\tau_f \leqslant 10$, and for $P_T \geqslant 0.04$ μM in Fig. 5(c), which corresponds to $\tau_r/\tau_f \leqslant 1.5$. The fitting is not good when $\tau_r/\tau_f > 10$ but not large enough as in Fig. 5(b) for $P_T < 0.15$ μM or in Fig. 5(c) for $P_T < 0.04$ μM. In this region, the fitting tends to overestimate the diffusion coefficient $\tilde{D}_2$ [e.g., the corresponding points in Fig. 5(c) fall outside the frame of the figure].

D. Transition from free to effective diffusion coefficients in experiments

The transition from the fast reaction to the fast diffusion limit was explored so far by changing the off reaction rate $k_{\rm off}$. Similar global changes in the ACF are obtained when other parameters that affect the ratio of time scales are changed [15,31]. For example, varying the volume of observation changes the particle diffusion characteristic time $\tau_f = w_r^2/4D_f$, and in this way the best analytic approximation to the ACF can be changed. In particular, we did obtain similar changes to the ones discussed so far when the full ACF was computed using the parameters of Table I, $k_{\rm off} = 1$ s^{-1} and $0.1 \leqslant w_r \leqslant 20$ μm (data not shown). On fitting the obtained ACFs with Eq. (6), the free particle diffusion coefficient D_f was recovered for $w_r^2 k_{\rm off} \geqslant 0.25$ μm^2/s and the collective coefficient D_u was recovered for $w_r^2 k_{\rm off} \geqslant 25$ μm^2/s (for which $\tau_f \sim \tau_r$) (data not shown). The question arises of whether it is possible to perform experiments with different values of w_r and, in this way, estimate both free and effective coefficients and derive information on the reactions. Reduction in the observation volume to reach the fast diffusion limit is not always possible. Enlargement of the volume, on the other hand, is more feasible and the fast reaction limit can also give meaningful information. On the other hand, obtaining an ACF with a shape that changes noticeably with the observation volume is *per se* very informative. The question that arises then is to what extent the volume can be enlarged and the autocorrelation of the fluctuations can still be computed. According to the exploration with varying w_r described before the transition to D_u is observed for $w_r^2 k_{\rm off} \sim 0.25$ μm^2/s. This transition point would correspond to $w_r \sim 0.5$ μm (a value of the order of the typical one obtained with a confocal microscope) for $k_{\rm off} \sim 100$/s and to twice this value, $w_r \sim 1$ μm, for $k_{\rm off} \sim 25$/s. Given the concentrations of our example, the number of fluorescent particles in the observation volume $5\pi^{3/2} w_r^3 P_T$ would then be 73 and 584, respectively, which are adequate for FCS experiments (see, e.g., [32]).

In order to probe in a more realistic setting whether the observation volume can be enlarged and still give rise to an informative ACF we have performed stochastic simulations as explained in Sec. II. We show the results in Fig. 6 where we have plotted the ACFs obtained from these simulations using $k_{\rm off} = 35$ s^{-1} and different values of w_r ($w_r = 0.3$, 0.5, 0.8, and 1.2 μm). There we observe that fluctuations are large enough in all cases probed to allow computation of an informative ACF. On introducing a rescaling factor so that all curves span the same region of the plot, the transition between two types of regimes is noticeable in Fig. 6(a). It then is clear from Figs. 6(b) and 6(c), where we have plotted the ACF for $w_r = 0.3$ μm and $w_r = 1.2$ μm, respectively, that the shortest time scale that can be estimated with the fitting (τ_1) changes and can be extracted in both cases. Obtaining the longest time scale (the one that corresponds to the free diffusion of the traps) is more complicated for $w_r = 1.2$ μm because the ACF is very noisy in this region of τ. The values τ_1 and τ_2 shown in Figs. 6(b) and 6(c) were obtained by fitting the "noiseless" ACF

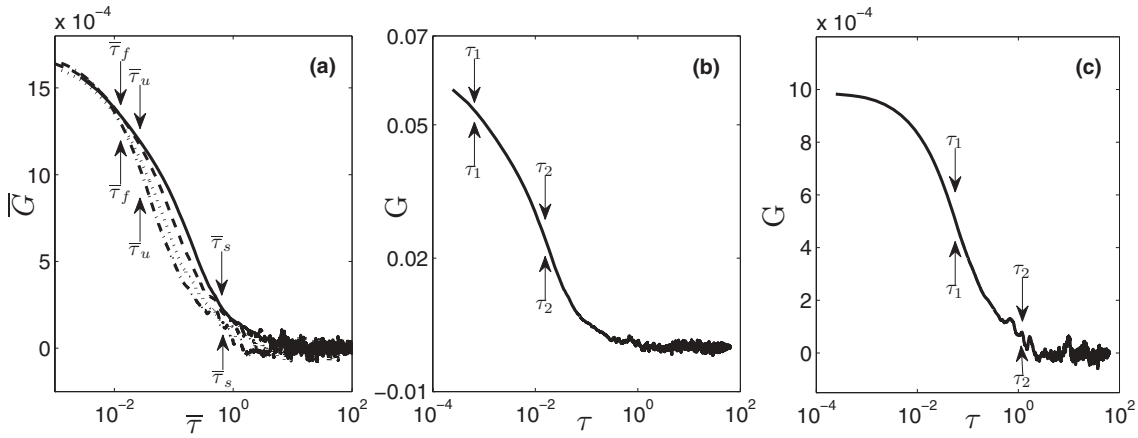

FIG. 6. Autocorrelation functions obtained from stochastic simulations performed with the parameters of Table I, $k_{\rm off} = 35\ {\rm s}^{-1}$ and different values of w_r. (a) Rescaled ACFs $\overline{G} \equiv w_r^3 G(\tau)$, as functions of the rescaled "time" $\overline{\tau} \equiv \tau w_r^2$ for $w_r = 0.3\ \mu$m (solid line), 0.5 μm (dashed line), 0.8 μm (dotted line), and 1.2 μm (dash-dotted line). Three relevant times, $\overline{\tau}_f = 1/4D_f$, $\overline{\tau}_u = 1/4D_u$, and $\overline{\tau}_s = 1/4D_S$ are indicated with arrows. (b) $G(\tau)$ for $w_r = 0.3\ \mu$m. (c) $G(\tau)$ for $w_r = 1.2\ \mu$m. τ_1 and τ_2 are the fitted times obtained by fitting the noiseless ACF [Eqs. (A7)–(A10)] with Eq. (6). The transition between two types of regime as w_r is increased is noticeable.

[given by Eqs. (A7)–(A10)] with Eq. (6), and this problem does not arise. In any case, the stochastic simulations show that for certain parameter values ($k_{\rm off} \sim 10$–$100\ {\rm s}^{-1}$ in our example) one can infer whether the estimated coefficients are effective or free by enlarging the observation volume from the typical value in a confocal setup (with $w_r = 0.3\ \mu$m) to a larger one. Doing these simulations we have also confirmed that the theoretical expressions Eqs. (A7)–(A10) provide a good description of the autocorrelation function for the problem under study: the functions obtained with the stochastic simulations are noisy versions of the ACF obtained using Eqs. (A7)–(A10) (data not shown).

IV. DISCUSSION AND CONCLUSIONS

Diffusion is a key transport process inside cells. Having reliable estimates of diffusion coefficients *in situ* is thus most important. In the case of biological molecules, diffusion is usually hindered by other processes such as reactive interactions with binding sites. Depending on the relative time scales involved, the net resulting transport may be approximately diffusive but with "effective" (concentration-dependent) rather than "free" diffusion coefficients. In such a case, the transport rates estimated under certain conditions cannot readily be used to infer at what pace transport will occur under others. In order to overcome this problem one needs estimates of free diffusion coefficients and reaction rates separately and a biophysical model to eventually compute net transport rates under a variety of conditions.

FCS provides a noninvasive method to infer diffusion coefficients *in situ* and, in certain cases, reaction rates as well [15,18]. In order to determine these quantities from experiments it is necessary to have a simple parametrized expression for the fluorescence ACF, something that is not always possible when the fluorescent particles react with other (unobservable) species. In [11] an analytic expression was derived for the ACF in the fast reaction limit and when these other species were in excess. The fast reaction limit was also studied in [17,18,23] without the assumption that the binding sites were in excess. The ACF can also be approximated analytically under the assumption of fast enough diffusion [15] in which case free diffusion coefficients can, in principle, be derived. In [15] the two limiting cases were compared. In the present paper we have explored the transition between the fast reaction and the fast diffusion limits. We have also studied the ACF in the fast reaction limit when the relationship between the binding sites and the free particle concentrations varies between a situation in which the binding sites are saturated and another one in which they are barely occupied.

The studies reported in the present paper were performed within the framework of a simple biophysical model but their consequences can be extended to more complicated ones. Based on this biophysical model in which fluorescent particles diffuse and interact with a single type of binding site, we computed numerically the theoretical ACF with no approximations for a wide range of values of the reaction rate $k_{\rm off}$. In this way we explored its behavior for different ratios between the diffusion [$\tau_f = w_r^2/(4D_f)$] and the reaction [$\tau_r = 1/(k_{\rm off} + k_{\rm on}P_{feq} + k_{\rm on}S_{eq})$] time scales (Fig. 1). We subsequently tried to fit it with different expressions [Eqs. (6)–(8)]. The results of all these fittings agreed with the fast diffusion approximation [Eq. (6) with $\tilde{D}_1 = D_S$ and $\tilde{D}_2 = D_f$ where D_S and D_f are the free diffusion coefficients of the binding sites and the fluorescent particles, respectively] for $k_{\rm off} \leqslant 0.1/{\rm s}$ ($\tau_f/\tau_r \leqslant 6.23 \times 10^{-4}$) and with the fast reaction approximation [Eq. (6) with $\tilde{D}_1 = D_S$ and $\tilde{D}_2 = D_u$ with D_u the "collective" effective coefficient D_u given by Eq. (3)] for $k_{\rm off} \geqslant 10^4/{\rm s}$ ($\tau_f/\tau_r \geqslant 62.3$). In between the two extreme situations, fitting the ACF with the superposition of three components given by Eq. (7) gave the smallest differences. However, this did not always mean an improvement in the estimates of the diffusion coefficients. In particular, for $k_{\rm off} = 1000/{\rm s}$ ($\tau_r/\tau_f = 0.16$) none of the coefficients obtained with this fitting corresponded to an actual coefficient of the

problem, while the results obtained with (6) or (8) agreed with those of the fast reaction approximation. Furthermore for $10/\mathrm{s} \leqslant k_{\mathrm{off}} \leqslant 100/\mathrm{s}$ the fitting with Eq. (7) failed to find a term with the free binding site coefficient D_S, which, as explained in the Appendix, should always be present. Fitting with two purely diffusive components [Eq. (6)], on the other hand, always gave one meaningful coefficient $\tilde{D}_2$, which was either approximately equal to D_f (for $k_{\mathrm{off}} \leqslant 10/\mathrm{s}$ for which $\tau_r/\tau_f \geqslant 16$) or to D_u (for $k_{\mathrm{off}} \geqslant 100/\mathrm{s}$ for which $\tau_r/\tau_f \leqslant 1.6$). Therefore, the collective coefficient D_u may be derived from the ACF even if the reaction characteristic time is of the same order as the diffusion one, $\tau_r/\tau_f \leqslant 1.6$. The other coefficient obtained with Eq. (6) was of the order of D_S for all values of k_{off} with the exception of $k_{\mathrm{off}} = 10/\mathrm{s}$ and $k_{\mathrm{off}} = 100/\mathrm{s}$ (for which $1.6 \leqslant \tau_r/\tau_f \leqslant 16$). Fitting with the anomalous diffusion model, Eq. (8), on the other hand, gave the worst results with regard to the meaning of the diffusion coefficients.

In order to understand how the ACF reduces to a two-component expression even though, as explained in the Appendix, it is characterized by three eigenvalues, we analyzed how its three components varied when going from one extreme situation to the other (Fig. 3). We observed that, in the fast diffusion limit, two of the components are characterized by the same characteristic time ($\tau = w_r^2/4D_S$). The other component has the smallest correlation time, which is the one associated with the particle free diffusion coefficient D_f. In the fast reaction limit the weight of the component with the smallest correlation time becomes negligible, and we are left with two terms with correlation times associated with D_S and with the effective diffusion coefficient, D_u. The fast diffusion limit holds while $\tau_r/\tau_f \geqslant 160$. The fast reaction limit holds while $\tau_r/\tau_f \leqslant 0.16$. However, as we mentioned before, the free particle diffusion coefficient (typical of the fast diffusion limit) can be obtained for $\tau_r/\tau_f \geqslant 16$ and the effective diffusion D_u (typical of the fast reaction limit) can be obtained for $\tau_r/\tau_f \leqslant 1.6$ when fitting with two purely diffusive components.

An important difference between the coefficients that may be derived in the fast diffusion and in the fast reaction limits, D_f and D_u, is that the latter is concentration dependent while the former is not. We confirmed this different behavior by analyzing situations with different values of the concentration of fluorescent particles P_T (Fig. 4). We also showed that the coefficient derived in the fast reaction limit is the collective coefficient defined in Eq. (3). This differs from the weighted average between D_f and D_S that defines the single-molecule effective coefficient D_t given by Eq. (2). As described in [3] D_t and D_u can be arbitrarily different from each other. Having the correct expression for the effective coefficient is key to interpreting FCS results [29]. In a model like the one we are analyzing here but where fluorescent and nonfluorescent particles coexist, the ACF gives both D_t and D_u in the fast reaction limit [23]. This suggests that by partially photobleaching the sample one could change the relative weights of the different terms of the ACF and, in this way, extract more information about the system under study. Our exploration of the model for varying concentrations confirms that even when τ_r is slightly larger than τ_f ($\tau_r/\tau_f \sim 1.5$) fitting with two diffusive components gives relatively accurate information on the effective diffusion coefficient D_u (see Fig. 5). It also shows that, even in the fast reaction limit, the free diffusion coefficient D_f can be recovered, depending on the relative concentrations of the reactants at work. As a result of all these explorations we conclude that fitting with purely diffusive components gives relatively accurate information on meaningful diffusion coefficients even outside the conditions for which the fast diffusion or the fast reaction limit holds.

The transition from the fast reaction to the fast diffusion limit was first explored by changing the off reaction rate k_{off}. We then analyzed it by changing w_r (i.e., the size of the illumination volume). In recent years several modifications to the traditional FCS setup have been explored [20], some of which were aimed at reducing the observation volume, a desirable goal since free rather than effective coefficients could then be inferred. The observation volume can be reduced, for example, using multiphoton excitation [12,14], metallic nanoparticles that can locally enhance the illumination intensity [33], or total internal reflection illumination [31]. However, these methods are not always readily applicable. In order to study how the results of FCS experiments change with the ratio of time scales and determine if effective or free coefficients are estimated, one could also enlarge the observation volume. We have explored this possibility using both Eqs. (A7)–(A10) and stochastic simulations to compute the ACF. From the former we concluded that the effective diffusion coefficient is recovered for $w_r^2 k_{\mathrm{off}} \geqslant 25\ \mu\mathrm{m}^2/\mathrm{s}$. From the stochastic simulations we concluded that for realistic parameter values (i.e., those of Table I with $k_{\mathrm{off}} \sim 10$–$100\ \mathrm{s}^{-1}$) the size of the beam waist w_r can be enlarged from a typical confocal value $0.3\ \mu\mathrm{m}$ to a larger one (also achievable in a confocal microscope) $w_r \sim 1.2\ \mu\mathrm{m}$, and still obtain a set of ACFs where the transition between the fast diffusion and the fast reaction limits can be observed. Furthermore, the largest coefficient (the one that goes from free to effective) can be estimated in both cases. Thus, this gives a way to identify, under certain conditions, whether the estimated coefficient is free or effective and whether or not care should be taken in using it under other concentration conditions. Another way by which the relationship between the two relevant time scales can be changed is by varying some concentration which changes the reaction time scale. This is not always possible in real systems. However, there are problems in which the substance of interest is distributed nonuniformly in space. This is exactly what happens in the case of the Bicoid protein in embryos of *D. melanogaster* [34]. Namely, there is a gradient of Bicoid along the embryo which is key to establishing the dorsal-ventral axis. The rate at which Bicoid diffuses in the embryo has been probed at the anterior pole by means of FRAP [25] and FCS [24] experiments. The natural nonuniform distribution of Bicoid provides a natural setting in which to explore changes in the ACF and, from its fitting, derive more information on the system under study [29].

ACKNOWLEDGMENTS

This research has been supported by UBA (Grant No. UBACyT 20020100100064), ANPCyT (Grants No. PICT 2010-1481 and No. PICT 2010-2767) and CONICET (Grant No. PIP 5131).

APPENDIX

We consider the simplest possible model with species that diffuse and react, some of which are fluorescent. Namely, we assume that there are three species: free particles P_f, "traps" or binding sites S, and bound particles P_b that interact according to the scheme given by Eq. (1) and diffuse with free coefficients D_f, D_S, and D_S, respectively. It is implicit in the latter that S is massive enough so that the diffusion rate of a single S molecule or of a bound particle P_b is the same. We further assume that the species P_f and P_b are fluorescent. The evolution equations for the concentrations $[P_f]$, $[P_b]$, and $[S]$ are then given by

$$\begin{aligned}\frac{\partial[P_f]}{\partial t} &= D_f\nabla^2[P_f] - k_{\text{on}}[P_f][S] + k_{\text{off}}[P_b],\\ \frac{\partial[P_b]}{\partial t} &= D_S\nabla^2[P_b] + k_{\text{on}}[P_f][S] - k_{\text{off}}[P_b],\\ \frac{\partial[S]}{\partial t} &= D_S\nabla^2[S] - k_{\text{on}}[P_f][S] + k_{\text{off}}[P_b].\end{aligned} \tag{A1}$$

In FCS experiments, fluctuations around an equilibrium situation, $P_{feq} \equiv \langle[P_f]\rangle$, $P_{beq} \equiv \langle[P_b]\rangle$, and $S_{eq} \equiv \langle[S]\rangle$, are analyzed. At equilibrium, the concentrations P_{feq}, P_{beq} and S_{eq} are uniformly distributed (for FCS it suffices that they be uniform over the observation volume) and satisfy

$$P_{feq}S_{eq} = K_D P_{beq}, \quad P_{feq} + P_{beq} = P_T, \quad S_{eq} + P_{beq} = S_T, \tag{A2}$$

where $K_D \equiv k_{\text{off}}/k_{\text{on}}$ and P_T and S_T are the total concentrations of particles and binding sites, respectively.

To determine the dynamics of the fluctuations, Eqs. (A1) are linearized around the equilibrium solution. The solutions to these linearized equations are then computed in Fourier space and written in terms of branches of eigenvalues $\lambda(\mathbf{q})$ and eigenvectors $\chi(\mathbf{q})$, where $\mathbf{q}$ is the wave number vector, i.e., the variable in Fourier space conjugate to the spatial coordinate $\mathbf{r}$ [13,23]. The linearized dynamics also prescribes how, under a small perturbation, the system decays back to the equilibrium solution. In particular, at long times the dynamics of P_f is dominated by the so-called "collective" effective diffusion coefficient [3] given by Eq. (3). This is different from the "single-particle" effective diffusion coefficient [3] given by Eq. (2) which enters the constant of proportionality between the mean square displacement of a single marked particle and the time elapsed. Both coefficients play a relevant role when reactions occur on a faster time scale than free diffusion. The fact that S is significantly more massive than P_f implies that $D_S < D_f$ which, in turn, yields $D_t/D_u \leqslant 1$. Given an equilibrium situation, this ratio can be arbitrarily small depending on the values of the equilibrium concentrations and the dissociation constant [3].

FCS monitors fluorescence fluctuations in a small observation volume which is determined by how the sample is illuminated. The intensity distribution of the illumination spot is usually approximated by

$$I(\mathbf{r}) = I(0)e^{-2r^2/w_r^2}e^{-2z^2/w_z^2}, \tag{A3}$$

where $I(0)$ is the illumination intensity at $\mathbf{r} = 0$, (r,z) are cylindrical coordinates with z the spatial coordinate along the beam propagation direction, and r the radial coordinate in the perpendicular plane. w_z and w_r are the sizes of the beam waist along z and r, respectively; in general, $w_z > w_r$. The fluorescence collected from the illuminated volume at any given time, $F(t)$, is then related to the number of fluorescent molecules that are inside the volume at that time. To be more specific, in the case of the simple model introduced in Sec. I, $F(t)$ is given by

$$F(t) = \int QI(\mathbf{r})\{[P_f](\mathbf{r},t) + [P_b](\mathbf{r},t)\}d^3r, \tag{A4}$$

if both free and bound particles have the same photophysical properties. In (A4) the concentrations are computed at time t and spatial point $\mathbf{r}$, and the parameter Q takes into account the detection efficiency, the fluorescence quantum yield, and the absorption cross section at the wavelength of excitation of all the fluorescent particles.

Fluctuations around the mean fluorescence $\langle F(t)\rangle$ are characterized by the time-averaged autocorrelation function, which is given by

$$G(\tau) = \frac{\langle\delta F(t)\delta F(t+\tau)\rangle}{\langle F(t)\rangle^2}, \tag{A5}$$

where $\delta F(t) = F(t) - \langle F(t)\rangle$. If P_f and P_b were two independent species that diffused freely with coefficients D_f and D_S, respectively, and did not interact through the reaction (1), $G(\tau)$ would be of the form

$$G(\tau) = \frac{G_{o_f}}{\left(1+\frac{\tau}{\tau_f}\right)\sqrt{1+\frac{\tau}{w^2\tau_f}}} + \frac{G_{o_b}}{\left(1+\frac{\tau}{\tau_S}\right)\sqrt{1+\frac{\tau}{w^2\tau_S}}} \tag{A6}$$

with $V_{\text{eff}} = \pi^{3/2}w_r^2w_z$ the effective sampling volume; $\tau_f = w_r^2/(4D_f)$ and $\tau_S = w_r^2/(4D_S)$ the characteristic diffusion times of both species across the sampling volume; $w = w_z/w_r$ the ratio of widths along the axial and perpendicular directions, respectively; and $G_{o_f} = P_{feq}/V_{\text{eff}}P_T^2$ and $G_{o_b} = P_{beq}/V_{\text{eff}}P_T^2$ the weights. For the model considered here, for which the dynamics is described by Eq. (A1), Eq. (A6) holds only in the limit of fast diffusion ($\tau_r^{-1} \equiv k_{\text{off}} + k_{\text{on}}P_{feq} + k_{\text{on}}S_{eq} \ll \tau_f^{-1} \equiv 4D_f/w_r^2$) [15]. Outside this limit, it is usually impossible to have an algebraic expression for $G(\tau)$. In such cases it is useful to work in terms of the eigenvectors and eigenvalues of the linearized version of Eqs. (A1) in order to compute $G(\tau)$.

Following [13] we assume that the correlation length is much smaller than the distance between fluorescent particles so that fluctuations in the concentrations of the fluorescent species ($\delta C_1 \equiv [P_f] - P_{feq}$, $\delta C_2 \equiv [P_b] - P_{beq}$) satisfy $\langle\delta C_j(\mathbf{r},t)\delta C_k(\mathbf{r},t)\rangle \propto \delta_{jk}\delta(\mathbf{r}-\mathbf{r}')$, $1 \leqslant j,k \leqslant 2$. Furthermore, assuming that fluctuations in the number of fluorescent particles of a given species follow a Poisson distribution [13], i.e., that $\langle\delta C_j(\mathbf{r},t)\delta C_k(\mathbf{r},t)\rangle = \langle C_j\rangle\delta_{jk}\delta(\mathbf{r}-\mathbf{r}')$, $1 \leqslant j,k \leqslant 2$, $G(\tau)$ can be written as the sum of three terms each of which corresponds to a different branch of eigenvalues of the linearized version of Eqs. (A1). Namely, as shown in [23] $G(\tau)$

reads

$$G(\tau) = G_1(\tau) + G_2(\tau) + G_3(\tau), \tag{A7}$$

$$G_1(\tau) = \frac{G_{os}}{\left(1+\frac{\tau}{\tau_S}\right)\sqrt{1+\frac{\tau}{w^2\tau_S}}}, \tag{A8}$$

$$G_2(\tau) = \frac{P_{feq}}{4hk_{\text{off}}P_T^2}\int \frac{d^3\mathbf{q}}{(2\pi)^3} e^{-W(q)+\hat{\lambda}_2\tau k_{\text{off}}} \times \left(2\nu + \sqrt{\cdot} + \frac{\nu^2-(D_S-D_f)^2q^4}{\sqrt{\cdot}}\right), \tag{A9}$$

$$G_3(\tau) = \frac{P_{feq}}{4hk_{\text{off}}P_T^2}\int \frac{d^3\mathbf{q}}{(2\pi)^3} e^{-W(q)+\hat{\lambda}_3\tau k_{\text{off}}} \times \left(2\nu - \sqrt{\cdot} - \frac{\nu^2-(D_S-D_f)^2q^4}{\sqrt{\cdot}}\right), \tag{A10}$$

where

$$G_{os} = \frac{P_{beq}^2}{V_{\text{eff}}P_T^2 S_T}, \tag{A11}$$

with V_{eff} the effective sampling volume and $\tau_S = w_r^2/(4D_S)$, as before; $W(\mathbf{q}) \equiv w_r^2q_r^2/4 + w_z^2q_z^2/4$ with q_r and q_z the variables in Fourier space that are conjugate to r and z, respectively, $q^2 = q_r^2 + q_z^2$ is the wave number squared, $\{\hat{\lambda}_i\}_{i=1}^3$ are dimensionless versions of the (branches of) eigenvalues of the linearized reaction-diffusion problem that can be written as

$$\begin{aligned}
\hat{\lambda}_1 &= -\frac{D_S}{k_{\text{off}}}q^2,\\
\hat{\lambda}_2 &= -\frac{1}{2}\left[a+h+\left(\frac{D_S}{k_{\text{off}}}+\frac{D_f}{k_{\text{off}}}\right)q^2\right] + \frac{1}{2D_f}\sqrt{\cdot},\\
\hat{\lambda}_3 &= -\frac{1}{2}\left[a+h+\left(\frac{D_S}{k_{\text{off}}}+\frac{D_f}{k_{\text{off}}}\right)\hat{q}^2\right] - \frac{1}{2D_f}\sqrt{\cdot},
\end{aligned} \tag{A12}$$

with $\sqrt{\cdot} = [(D_S-D_f)^2q^4 + 2q^2(D_S-D_f)k_{\text{off}}(h-a) + \nu^2]^{1/2}$, $\nu = k_{\text{off}}(a+h)$, $a \equiv S_{eq}/K_D$, and $h \equiv S_T/S_{eq}$. Assuming that the fluctuations do not initially obey the Poisson statistics changes the weights but not the time scales of the components. The time dependence, however, is approximately diffusive only in certain limits.

Under the above mentioned assumptions, the value of the ACF at $\tau = 0$, $G_o \equiv G(\tau = 0) = 1/(V_{\text{eff}}P_T)$, i.e., it is inversely proportional to the number of fluorescent particles in the observation volume. Another property is that the term corresponding to the first eigenvalue G_1 can be integrated analytically. It is a purely diffusive term with the free diffusion coefficient of the binding sites, D_S. The other two eigenvalues do not correspond to a purely diffusive transport at all times or length scales. However, one of them corresponds to diffusion in the long time or long wavelength ($q \to 0$) limits, while the other one does not. Namely, from Eq. (A12) it is possible to show that the dimensional eigenvalues satisfy

$$\lambda_1 = -D_Sq^2, \quad \lambda_2 \approx -D_uq^2, \quad \lambda_3 \approx -\nu_{uu} - D_{uu}q^2, \tag{A13}$$

with

$$\nu_{uu} = (a+h)k_{\text{off}}, \quad D_{uu} = \frac{aD_f + hD_S}{a+h}, \tag{A14}$$

as $q \to 0$.

The limiting behavior expressed by Eqs. (A13) and (A14) has been used in [23] to approximate the ACF by an analytic expression the limit of fast reactions (i.e., $\tau_r^{-1} \gg \tau_f^{-1}$). In this limit the ACF can be approximated by [23]

$$G(\tau) = \frac{G_{os}}{\left(1+\frac{\tau}{\tau_S}\right)\sqrt{1+\frac{\tau}{w^2\tau_S}}} + \frac{G_{oef}}{\left(1+\frac{\tau}{\tau_{ef}}\right)\sqrt{1+\frac{\tau}{w^2\tau_{ef}}}}, \tag{A15}$$

where G_{os} and τ_S are the same as before, $\tau_{ef} = w_r^2/(4D_u)$, and G_{oef} is given by

$$G_{oef} = \frac{1}{V_{\text{eff}}P_T} - \frac{P_{beq}^2}{V_{\text{eff}}P_T^2S_T}. \tag{A16}$$

We see in Eq. (A15) that the third component of the ACF is lost in this limit. The two terms that remain have the same functional form as those of Eq. (A6). The first term has the characteristic time $\tau_S = w_r^2/(4D_S)$ which corresponds to the binding site diffusion time across the sampling volume. The second term has a time scale $\tau_{ef} = w_r^2/(4D_u)$ associated with the collective effective diffusion coefficient D_u of Eq. (3), which depends on the free diffusion coefficients of particles and binding sites and on the reaction parameters.

[1] H. C. Berg, *Random Walks in Biology* (Princeton University Press, Princeton, NJ, 1993).
[2] J. Wagner and J. Keizer, Biophys. J. **67**, 447 (1994).
[3] B. Pando, S. P. Dawson, D.-O. D. Mak, and J. E. Pearson, Proc. Natl. Acad. Sci. **103**, 5338 (2006), http://www.pnas.org/content/103/14/5338.full.pdf+html.
[4] D. E. Strier and S. P. Dawson, J. Chem. Phys. **112**, 825 (2000).
[5] G. Smith, Biophys. J. **71**, 3064 (1996).
[6] A. Duffy, J. Sneyd, and P. Dale, SIAM J. Appl. Math. **58**, 1178 (2001).
[7] D. E. Strier, A. Chernomoretz, and S. P. Dawson, Phys. Rev. E **65**, 046233 (2002).
[8] D. Axelrod, D. E. Koppel, J. Schlessinger, E. Elson, and W. W. Webb, Biophys. J. **16**, 1055 (1976).
[9] K. Jacobson and J. Wojcieszyn, Proc. Natl. Acad. Sci. USA **81**, 6747 (1984).
[10] P. Gribbon and T. E. Hardingham, Biophys. J. **75**, 1032 (1998).
[11] D. Magde, E. Elson, and W. W. Webb, Phys. Rev. Lett. **29**, 705 (1972).
[12] K. Berland, P. So, and E. E Gratton, Biophys. J **68**, 694 (1995).
[13] O. Krichevsky and G. Bonnet, Rep. Prog. Phys. **65**, 251 (2002).
[14] P. Schwille, U. Haupts, S. Maiti, and W. W. Webb, Biophys. J **77**, 2251 (1999).
[15] E. L. Elson, Traffic **2**, 789 (2001).

[16] S. A. Kim and P. Schwille, Curr. Opin. Neurobiol. **13**, 583 (2003).
[17] D. Grünwald, M. C. Cardoso, H. Leonhardt, and V. Buschmann, Curr. Pharm. Biotechnol. **6**, 381 (2005).
[18] E. Bismuto, E. Gratton, and D. C. Lamb, Biophys. J. **81**, 3510 (2001).
[19] M. A. Digman, P. Sengupta, P. W. Wiseman, C. M. Brown, A. R. Horwitz, and E. Gratton, Biophys. J **88**, L33 (2005).
[20] E. Haustein and P. Schwille, Annu. Rev. Biophys. Biomol. Struct. **36**, 151 (2007).
[21] B. Sprague, R. Pego, D. Stavreva, and J. McNally, Biophys. J. **86**, 3473 (2004).
[22] B. Sprague and J. McNally, Trends Cell Biol. **15**, 84 (2005).
[23] L. Sigaut, M. L. Ponce, A. Colman-Lerner, and S. P. Dawson, Phys. Rev. E **82**, 051912 (2010).
[24] A. Abu-Arish, A. Porcher, A. Czerwonka, N. Dostatni, and C. Fradin, Biophys. J. **99**, L33 (2010).
[25] T. Gregor, E. F. Wieschaus, A. P. McGregor, W. Bialek, and D. W. Tank, Cell **130**, 141 (2007).
[26] T. Gregor, D. W. Tank, E.F. Wieschaus, and W. Bialek, Cell **130**, 153 (2007).
[27] Computer code MATLAB, version 7.10.0 (R2010a) (The MathWorks Inc., Natick, MA, 2010).
[28] L. Sigaut, Ph.D. thesis, Departamento de Fisica, FCEN, Universidad de Buenos Aires, 2011.
[29] L. Sigaut, J. E. Pearson, A. Colman-Lerner, and S. Ponce Dawson (unpublished).
[30] D. S. Banks and C. Fradin, Biophys. J. **89**, 2960 (2005).
[31] N. L. Thompson, P. Navaratnarajah, and X. Wang, J. Phys. Chem. B **115**, 120 (2011).
[32] S. Charier, A. Meglio, D. Alcor, E. Cogné-Laage, J. Allemand, L. Jullien, and A. Lemarchand, J. Chem Soc. A **127**, 15491 (2005).
[33] L. Estrada, M. Roberti, S. Simoncelli, V. Levi, P. Aramendía, and O. Martínez, J. Phys. Chem. B **116**, 2306 (2012).
[34] W. Driever and C. Nussleinvolhard, Cell **54**, 83 (1988).